Published in final edited form as:

J Urol. 2019 February ; 201(2): 332–341. doi:10.1016/j.juro.2018.09.028.

Histological Validation of ^{11}Carbon-Acetate Positron Emission Tomography/Computerized Tomography in Detecting Lymph Node Metastases in Prostate Cancer

Nieroshan Rajarubendra,

Fabio Almeida,

Zarko Manojlovic,

Chisato Ohe,

Nariman Ahmadi,

Giovanni Cacciamani,

Michael Qiu,

Andre Abreu,

Jie Cai,

Gus Miranda,

Mariana C. Stern,

John Carpten,

Peter Kuhn,

Mahul B. Amin,

Parkash S. Gill,

Manju Aron,

Inderbir S. Gill*

USC Institute of Urology, Catherine and Joseph Aresty Department of Urology (NR, CO, NA, GC, MQ, AA, JCai, GM, MCS, ISG), Institute of Translational Genomics (NR, ZM, JCar), Department of Aerospace, Mechanical and Biomedical Engineering, Viterbi School of Engineering (PK), Department of Biological Sciences, Dornsife College of Letters, Arts and Sciences (PK), and Departments of Medicine, Pathology and Urology (PSG), Pathology (MA) and Preventive Medicine (MCS), Keck School of Medicine, University of Southern California, Los Angeles, California, Phoenix Molecular Imaging (FA), Phoenix, Arizona, and Department of Pathology, University of Tennessee (MBA), Memphis, Tennessee

Abstract

*Correspondence: 1441 Eastlake Ave., Suite No. 7416, Los Angeles, California 90089 (telephone: 323-865-3000; FAX: 323-865-2300; gillindy@gmail.com).

The corresponding author certifies that, when applicable, a statement(s) has been included in the manuscript documenting institutional review board, ethics committee or ethical review board study approval; principles of Helsinki Declaration were followed in lieu of formal ethics committee approval; institutional animal care and use committee approval; all human subjects provided written informed consent with guarantees of confidentiality; IRB approved protocol number; animal approved project number.

No direct or indirect commercial incentive associated with publishing this article.

Purpose: Conventional imaging cannot definitively detect nodal metastases of prostate cancer. We histologically validated ^{11}C-acetate positron emission tomography/computerized tomography to identify nodal metastases, examining prostate cancer factors that influence detection rates.

Materials and Methods: Patients with ^{11}C-acetate avid positron emission tomography/computerized tomography imaged pelvic/retroperitoneal lymph nodes underwent high extended robotic lymphadenectomy. A standardized mapping template comprising 8 predetermined anatomical regions was dissected during lymphadenectomy, allowing for matched, region based analysis and comparison of imaging and histological data.

Results: In 25 patients a total of 2,149 lymph nodes were excised (mean 86 per patient, range 27 to 136) and 528 (22%) harbored metastases (mean 21 positive nodes per patient, range 0 to 109). A total of 174 anatomical regions had matching imaging histological data. ^{11}C-acetate positron emission tomography/computerized tomography accurately identified 48 node-positive regions and accurately ruled out 88 regions as metastasis-free. ^{11}C-acetate sensitivity, specificity, and positive and negative predictive values were 67%, 84%, 74% and 79%, respectively. An increasing, histologically measured metastatic lesion size in long axis diameter of 5 or less, 6 to 10, 11 to 15, 16 to 20 and 21 mm or greater correlated with improved ^{11}C-acetate detection rates of 45%, 62%, 81%, 89% and 100%, respectively. Each standard uptake value unit increase correlated with a 1.9 mm increase in nodal long axis diameter ($p < 0.001$) and a 1.2 mm increase in short axis diameter ($p < 0.001$). Positive ^{11}C-acetate positron emission tomography/computerized tomography findings correlated with histological lymph node size (long axis diameter 12 mm and short axis diameter 6 mm), metastatic lesion size (long axis diameter 11 mm and short axis diameter 6 mm) and extranodal extension (positive 88% vs false-negative 58%, $p = 0.005$).

Conclusions: ^{11}C-acetate positron emission tomography/computerized tomography can identify prostate cancer metastatic nodal disease. However, it underestimates the true cephalad extent of nodal involvement, performing better in the pelvis than in the retroperitoneum. Standard uptake value, histological nodal size, intranodal metastasis size and extranodal extension correlate with cancer bearing nodes.

Keywords

prostatic neoplasms; lymph nodes; neoplasm metastasis; tomography; diagnostic imaging

IN PCa the detection of distant disease is crucial since metastatic disease is associated with 29% 5-year survival.[1] The anatomical location of metastatic disease has implications on outcomes since LN metastases have lower disease specific mortality rates compared to bone or visceral metastases.[2] This has led to more aggressive targeted treatment strategies in patients in whom imaging identified node-only metastatic disease to further improve outcomes in this subgroup of patients. Treatments such as surgical resection or targeted radiation therapy to tumor bearing nodes may improve survival and delay time to progression in certain patient populations.[3,4] At our institution we developed an extended rPLND and rRPLND technique in the setting of image identified node-only metastases of PCa.[5]

Suspicious lesions observed on routine CT/ magnetic resonance imaging can be further evaluated with PET using disease appropriate tracers, including those that detect metabolic

activity. The combination of PET and CT allows for anatomical as well as tracer activity evaluation of patients. One radiotracer used in PET, ^{11}C-acetate, has been studied in myocardial oxygen consumption cases as well as in some cancer cases, including PCa.

The acetate component of ^{11}C-acetate is metabolized into acetyl coenzyme A for fatty acid synthesis, which is incorporated into the intracellular phosphatidylcholine membrane at a higher level because tumor cells overexpress fatty acid synthetase.[6] The advantage of this tracer is that it is taken up in the pancreas, liver, spleen, salivary glands and bowel with no excretion into the urinary tract. The limitation to the widespread use of ^{11}C-acetate is its short half-life of 20 minutes, which requires treatment facilities to be equipped with a cyclotron on site.

Multiple radiotracers have been developed to detect metastatic PCa. However, there is controversy over which is most reliable and accurate as most are in the investigational/ validation phase. In this study we evaluated the performance of ^{11}C-acetate PET/CT as corroborated by the gold standard of anatomically matching histological data. This study correlates imaging with histology of a substantial number of LNs obtained from the pelvis and retroperitoneum using a standardized, defined anatomical template.

MATERIALS AND METHODS

Patients underwent combined rPLND and rRPLND in the primary or salvage setting when a prior ^{11}C-acetate PET/ CT image indicated the presence of lymph node-only metastases. There were no restrictions as long as the suspicious nodes were limited to the pelvis and the retroperitoneum (up to the level of the renal veins). Exclusion criteria were concurrent bony or visceral metastatic disease. Data were collected prospectively in our Institutional Review Board approved database (IRB No. HS-012030). Patients were consecutively recruited from the USC Institute of Urology, Keck School of Medicine, University of Southern California, from 2015 to 2017.

Robotic Pelvic Lymph Node Dissection and Retroperitoneal Lymph Node Dissection

Surgery was performed robotically with a da Vinci® Si™ or Xi Surgical System by a single, high volume robotic surgeon (ISG). A standardized lymphadenectomy template combining rPLND plus rRPLND was dissected, which extended from the renal vein/artery cranially to Cloquet's node caudally and bilaterally to the ureters. Clearance of the periaortic/caval, preaortic/caval, interaortocaval, retroaortic/caval, common/internal/external iliac vascular tree and presciatic fossa of Marseilles regions was achieved. The anatomical template was subdivided into 4 levels based on anatomical landmarks, including level I—encompassing LNs below the common iliac bifurcation, level II—from the upper limit of level I up to the aortic bifurcation, level III—from the upper limit of level II up to the inferior mesenteric artery, and level IV—from the upper limit of level III to the left renal vein crossing the aorta. Lymph nodes were sent for histological evaluation in multiple separate packets and indexed according to side specific anatomical template region.

^{11}C-Acetate Positron Emission Tomography/Computerized Tomography Acquisition and Assessment

Patients were positioned on an integrated Biograph 6 or Biograph 16 TruePoint™ PET/CT scanner. Radiotracer 740-1,480 MBq ^{11}C-acetate (half-life 20.3 minutes) was administered as an intravenous bolus.

First a CT scan was obtained from the vertex through to the pelvis. On the basis of the tomograph the tube current for the CT was adjusted utilizing a CARE Dose™ application to minimize exposure. The tube voltage was 130 kVP. After the CT scan emission images beginning at the pelvis and proceeding cranially were obtained 3 to 7 minutes after injection (mean 4.25).

Images were reconstructed with iterative reconstruction (2 iterations, 8 subsets, matrix 168 and a Gaussian filter).

Interpretation of the ^{11}C-acetate PET/CT was performed by a highly experienced nuclear medicine physician (FA). Since visualizing the inferior mesenteric artery on ^{11}C-acetate PET/CT is challenging, the bony landmark L3/L4 was used to differentiate levels III and IV. On ^{11}C-acetate imaging LNs were qualitatively deemed abnormal when increased metabolic activity was observed in enlarged or enlarging nodes compared to prior imaging. Sub cm nodes with mild metabolic activity were also considered positive if they were rounded and showed substantially higher activity than similarly sized physiological nodes in the inguinal region. The largest positive LN in each region was further characterized with the SAD, the LAD and the SUV (fig. 1). Postoperatively patients with a poor PSA response underwent repeat ^{11}C-acetate PET/CT to assess whether the initially identified LNs were excised.

Histopathological Assessment

Resected lymph node packets with adipose tissue were fixed in formalin and processed in accordance with the ADASP (Association of Directors of Anatomic and Surgical Pathology) recommendations.[7,8] Hematoxylin and eosin stained slides were reevaluated specifically for the purposes of this study by 2 specialized, genitourinary fellowship trained pathologists blinded to ^{11}C-acetate image data (MA and CO). The largest LN from each template region was measured for the SAD and the LAD. Metastatic cancer lesions in LNs were also measured for the SAD and the LAD, and examined for the presence of extranodal extension.

Statistical Analysis

Region based evaluation was done in areas with matching imaging and histopathological data sets. Multivariate linear regression modeling was performed with SAS®, version 9.0. Each stratified group was analyzed by the Mann-Whitney nonparametric test using GraphPad Prism™ 7.0a with $p < 0.05$ considered statistically significant.

RESULTS

A total of 25 patients met study eligibility criteria (table 1). Retroperitoneal rPLND plus rRPLND was performed in the salvage setting in 21 patients and in the primary setting in 4 who underwent robotic radical prostatectomy concomitantly with rPLND plus rRPLND.

Table 1 summarizes demographic data prior to ^{11}C-acetate PET/CT and rLND. Following rPLND plus rRPLND histological evaluation identified 2,149 excised LNs, of which 528 (22%) harbored metastatic disease (fig. 2). Thus, a mean of 86 LNs (range 27 to 132) was robotically excised per patient with 21 nodes (range 0 to 109) per patient harboring metastatic disease.

In the aggregate 174 separate regions had matching histological and ^{11}C-acetate imaging data (table 2 and fig. 3). In 26 regions there was no tissue to match with imaging due to severe scarring from previous resection and lack of nodal tissue. Overall 48 regions (28%) were imaging positive and histologically positive for cancer (TP), 14 (8%) were imaging positive but proved to be histologically negative (FP), 24 (14%) were imaging negative but histologically positive for cancer (false-negative) and 88 (50%) were imaging and histologically negative (negative). Thus, overall sensitivity was 67%, specificity was 84%, PPV was 74% and NPV was 79%. On per patient analysis the PPV of ^{11}C-acetate PET/CT was 84% with better detection rates in the pelvis than in the retroperitoneum (fig. 4).

Seven of the 25 patients (28%) had histologically confirmed metastatic deposits in 1 or more levels higher than the highest level predicted by ^{11}C-acetate PET/CT. This discrepancy was independent of PSA or PSA doubling time. Table 3 presents the correlation of imaging and histological data. Among various findings on ^{11}C-acetate PET/CT only SUV correlated with node positivity on histology and a SUV of 4 or greater uniformly identified metastatic nodes on histology (table 3). ^{11}C-acetate imaging positivity was influenced by histological nodal size, the size of the intranodal metastatic lesion and the presence of extranodal extension but there was considerable overlap between TP and false-negative image results (table 3). On ^{11}C-acetate PET/CT positive nodes were larger than negative nodes (table 4). Increasing histological metastatic node size had a linear correlation with ^{11}C-acetate positivity (table 4 and fig. 5).

Multivariate linear regression modeling of cancer lesion size after controlling for laterality, template level, Gleason score and prePET PSA demonstrated that for every unit increase in the SUV, the LAD increased by 1.9 mm (95% CI 1.5–2.2, $p < 0.001$) and the SAD increased by 1.2 mm (95% CI 1.0–1.4, $p < 0.001$). Strictly from a histological standpoint if retroperitoneal nodes were positive, pelvic nodes were always positive as well. In 2 patients level II nodes were positive despite negative level I nodes.

DISCUSSION

The use of imaging modalities and nomograms assists the clinician in predicting LN involvement of PCa and guide the extent of surgical resection.[9] Currently used imaging modalities (CT and magnetic resonance imaging) identify lesions mainly based on size criteria, lacking metabolic and functional assessment. As a result small, early nodal metastases may be missed. Prognostic prediction tools such as the Memorial Sloan Kettering Cancer Center or Briganti nomograms have been internally and externally validated with accuracy ranging from 77% to 82%.[10,11] However, Strandberg et al found that ^{11}C-acetate PET/CT was more accurate than a nomogram in predicting nodal metastases.[12]

The use of PET in urology is increasing, especially as new radiotracers have been developed with little or no urinary excretion. To our knowledge ours is the first study to corroborate PET/CT with extensive and standardized anatomical template LN mapping encompassing the retroperitoneum in PCa cases.

The absence of histological correlation, especially for false-negative anatomical regions, is a limitation of prior studies. In a study of LN dissection limited only to the common iliac arteries or lower a region based analysis showed that ^{11}C-acetate imaging had 27% to 62% sensitivity, 89% to 98% specificity, 62% to 74% PPV and 81% to 89% NPV.[13,14] Patient based analyses revealed slightly higher rates at 38% to 68% sensitivity, 78% to 96% specificity, 49% to 91% PPV and 62% to 89% NPV.[13,15,16] Our study had a PPV of 84%, which is commensurate with the literature.

When we assessed individual anatomical template levels, the sensitivity of the ^{11}C-acetate image decreased at higher levels. There were no differences in metastasis size or SUV in LNs in the pelvis or the retroperitoneum (supplementary table, http://jurology.com/). However, if multiple LNs in an anatomical chain are positive vs a single node, the chance of identifying avid nodes would be higher. As a result, tumor bulk, which is usually higher in the pelvis, influences the chances of lesion detection. This trend was also observed in our patient based analysis.

In our study the median SUV of FP and TP nodes was 2.3 and 3.2, respectively, with a SUV of 4 or higher always predicting a positive node. These SUV data are lower than in prior studies, which reported a median SUV of 5.2 to 5.3 for positive nodes.[17,18] Histologically median LADs and SADs of 12 and 6 mm for total node size, and 11 and 6 mm for intranodal metastatic lesion size, respectively, improved the chance of image detection. Interestingly extranodal extension was seen much more commonly in regions accurately identified by the image. These data indicate that positive PET/CT images correlate with larger nodal size and cancer volume as well as with extranodal extension. However, there is considerable overlap between TP and FP PET/CT images. The clinical implication of these data is that anatomical template based node dissection should be performed in patients with any node positivity on PET/CT. Removing only the PET/CT identified positive node risks leaving other image undetected positive nodes behind.

A positive correlation was seen between detection rates and the size of metastatic deposits in LNs. Cancer lesion sizes of 5 or less and 6 to 10 mm had 45% and 62% sensitivity, respectively. This was consistent with the literature as the accuracy is less reliable for lesions less than 10 mm.[19] The size of the metastatic lesion and, thus, its cancer burden is an important factor that increases the ^{11}C-acetate imaging yield, which may have implications on detecting early metastatic disease. On multivariate linear regression modeling for every unit increase in the SUV there was an increase of 1.9 mm in the LAD and 1.2 mm in the SAD of cancer lesion size. This underscores the importance of these 2 factors in accurately predicting nodal metastases.

The limitation of this study is our small, heterogeneous sample size. However, to our knowledge such detailed data from anatomical level based LN resection have not been

available to date, especially with matching imaging information. Since this type of major retroperitoneal surgery has the potential for high grade complications, only patients who had images indicating node-only disease were treated. To overcome selection bias we performed a region based analysis designed to compare matched imaging and pathology information.

A strength of our study is that a single experienced robotic surgeon performed similar, pre-planned, template based rPLND plus rRPLND in all patients and carefully labeled, individual nodal packets were evaluated histologically. ^{11}C-acetate PET/CT was able to identify LN only disease and exclude bony and visceral disease, which allowed for this select patient population to undergo surgery. This was seen in subsequent repeat images which did not show progression to bony or visceral disease.

The scope of the study was to validate the imaging modality with histological assessment. Oncologically 14 patients had a PSA response with a median reduction of 82%. Median followup was 11 months (range 1.9 to 18.9) during which 7 of the patients with a PSA reduction did not require any additional treatment.

Despite performing such substantial LN dissection, there remains the possibility that some LNs were not removed in the assigned template. In 4 patients with a post-rLND PSA rise repeat ^{11}C-acetate imaging demonstrated persistence of a single previously ^{11}C-acetate imaging identified, anatomical, avid lesion deep in the obturator fossa. This node could not be excised during rLND due to preexisting intense, fibrotic scarring from prior radical prostatectomy and/or primary radiation. In each of these 4 patients the residual hot spot was located in the level I region, including in the left obturator fossa in 3 and the presacral region in 1, deep in the pelvis, adjacent to bony and/or vascular landmarks and ensconced in dense fibrosis, making surgical excision technically dangerous. Thus, these 4 regions were excluded from analysis and the patients underwent focal, stereotactic radiotherapy as subsequent therapy. Not all patients were able to be re-imaged due to clinical indication or patient travel, which introduced some bias.

Management of high risk PCa involves multimodal therapy. This combination of imaging and resection when treating node-positive disease in PCa cases reduces or eliminates the need for whole pelvis and whole retroperitoneum radiation. With repeat imaging after postoperative inflammation has resolved focal radiotherapy, such as CyberKnife®, can be instituted only to the ^{11}C-acetate PET/CT positive site to minimize morbidity.

Our data indicate that ^{11}C-acetate imaging can identify patients with metastatic nodal disease with a high degree of accuracy (84% PPV) and it performs better in the pelvis than in the retroperitoneum. However, 28% of our patients had nodal metastases higher than the highest level identified by the image. Therefore, at least for the time being in these highly selected patients salvage LN dissection surgery should be planned in an anatomical template based manner rather than be strictly guided by the highest involved node identified on PET/CT. Further studies with long-term outcomes are needed to assess whether the performance of rRPLND plus rPLND in patients with imaging identified node-only recurrent PCa can materially and durably alter the natural history of PCa and its trajectory of metastatic progression.

CONCLUSIONS

Using ^{11}C-acetate imaging to detect node-only metastatic PCa is promising, performing better in the pelvis than in the retroperitoneum. Factors that increase the imaging detection of lymph node metastases include node size, metastatic deposit size, presence of extranodal extension and SUV. Since nodal metastases were present in regions not identified on imaging, template rPLND plus rRPLND in patients with positive images may be indicated rather than targeted resection of ^{11}C-acetate PET/CT positive sites only. Larger studies from other centers evaluating other radiopharmaceutical based images according to our study design are needed to document the accuracy of PET/CT to detect nodal involvement of PCa.

Supplementary Material

Refer to Web version on PubMed Central for supplementary material.

Abbreviations and Acronyms

CT	computerized tomography
FP	false-positive
LAD	long axis diameter
LN	lymph node
NPV	negative predictive value
PCa	prostate cancer
PET	positron emission tomography
PPV	positive predictive value
PSA	prostate specific antigen
rLND	retroperitoneal LN dissection
rPLND	robotic pelvic LN dissection
rRPLND	retroperitoneal rPLND
SAD	short axis diameter
SUV	standard uptake value
TP	true positive

REFERENCES

1. American Cancer Society: Cancer Facts and Figures 2017. Available at https://www.cancer.org/research/cancer-facts-statistics/all-cancer-facts-figures/cancer-facts-figures-2017.html. Accessed August 29, 2018.

2. Nini A, Gandaglia G, Fossati N et al. : Patterns of clinical recurrence of node-positive prostate cancer and impact on long-term survival. Eur Urol 2015; 68: 777. [PubMed: 25959166]
3. Tilki D, Mandel P, Seeliger F et al. : Salvage lymphnode dissection for nodal recurrence of prostate cancer after radical prostatectomy. J Urol 2015; 193: 484. [PubMed: 25180792]
4. Jereczek-Fossa BA, Fanetti G, Fodor C et al. : Salvagestereotactic body radiotherapy for isolated lymph node recurrent prostate cancer: single institution series of 94 consecutive patients and 124 lymph nodes. Clin Genitourin Cancer 2017; 15: e623. [PubMed: 28185875]
5. Abreu A, Fay C, Park D et al. : Robotic salvage retroperitoneal and pelvic lymph node dissection for 'node-only' recurrent prostate cancer: technique and initial series. BJU Int 2017; 120: 201.
6. Swinnen JV, Van Veldhoven PP, Timmermans Let al: Fatty acid synthase drives the synthesis of phospholipids partitioning into detergent-resistant membrane microdomains. Biochem Biophys Res Commun 2003; 302: 898. [PubMed: 12646257]
7. Association of Directors of Anatomic and Surgical Pathology: ADASP recommendations for processing and reporting lymph node specimens submitted for evaluation of metastatic disease. Am J Surg Pathol 2001; 25: 961. [PubMed: 11420470]
8. Berney DM, Wheeler TM, Grignon DJ et al. : International Society of Urological Pathology (ISUP) Consensus Conference on Handling and Staging of Radical Prostatectomy Specimens. Working group 4: seminal vesicles and lymph nodes. Mod Pathol 2011; 24: 39. [PubMed: 20818343]
9. Gandaglia G, Fossati M, Zaffuto E et al. : Development and internal validation of a novel model to identify the candidates for extended pelvic lymph node dissection in prostate cancer. Eur Urol 2017; 72: 632. [PubMed: 28412062]
10. Dell'Oglio P, Abdollah F, Suardi N et al. : Externalvalidation of the European Association of Urology recommendations for pelvic lymph node dissection in patients treated with robot-assisted radical prostatectomy. J Endourol 2014; 28: 416. [PubMed: 24188052]
11. Hinev AI, Anakievski D, Kolev NH et al. : Validation of nomograms predicting lymph node involvement in patients with prostate cancer undergoing extended pelvic lymph node dissection. Urol Int 2014; 92: 300. [PubMed: 24480972]
12. Strandberg S, Karlsson CT, Sundström T et al. : (11)C-acetate PET/CT in pre-therapeutic lymph node staging in high-risk prostate cancer patients and its influence on disease management—a retrospective study. EJNMMI Res 2014; 4: 55. [PubMed: 26116118]
13. Daouacher G, von Below C, Gestblom C et al. : Laparoscopic extended pelvic lymph node (LN) dissection as validation of the performance of [(11) C]-acetate positron emission tomography/computer tomography in the detection of LN metastasis in intermediate- and high-risk prostate cancer. BJU Int 2016; 118: 77. [PubMed: 26074275]
14. Schumacher MC, Radecka E, Hellström M et al. : [^{11}C]Acetate positron emission tomography-computed tomography imaging of prostate cancer lymph-node metastases correlated with histopathological findings after extended lymphadenectomy. Scand J Urol 2015; 49: 35. [PubMed: 25001948]
15. Haseebuddin M, Dehdashti F, Siegel BA et al. : ^{11}C-acetate PET/CT before radical prostatectomy: nodal staging and treatment failure prediction. J Nucl Med 2013; 54: 699. [PubMed: 23471311]
16. Almeida FD, Yen CK, Scholz MC et al. : Performance characteristics and relationship of PSA value/kinetics on carbon-11 acetate PET/CT imaging in biochemical relapse of prostate cancer. Am J Nucl Med Mol Imaging 2017; 7: 1. [PubMed: 28123863]
17. Leisser A, Pruscha K, Ubl P et al. : Evaluation offatty acid synthase in prostate cancer recurrence: SUV of [(11) C]acetate PET as a prognostic marker. Prostate 2015; 75: 1760. [PubMed: 26282590]
18. Budaüs L, Leyh-Bannurah SR, Salomon G et al. : Initial experience of (68)Ga-PSMA PET/CT imaging in high-risk prostate cancer patients prior to radical prostatectomy. Eur Urol 2016; 69: 393. [PubMed: 26116958]
19. Ganeshalingam S and Koh DM: Nodal staging. Cancer Imaging 2009; 9: 104. [PubMed: 20080453]

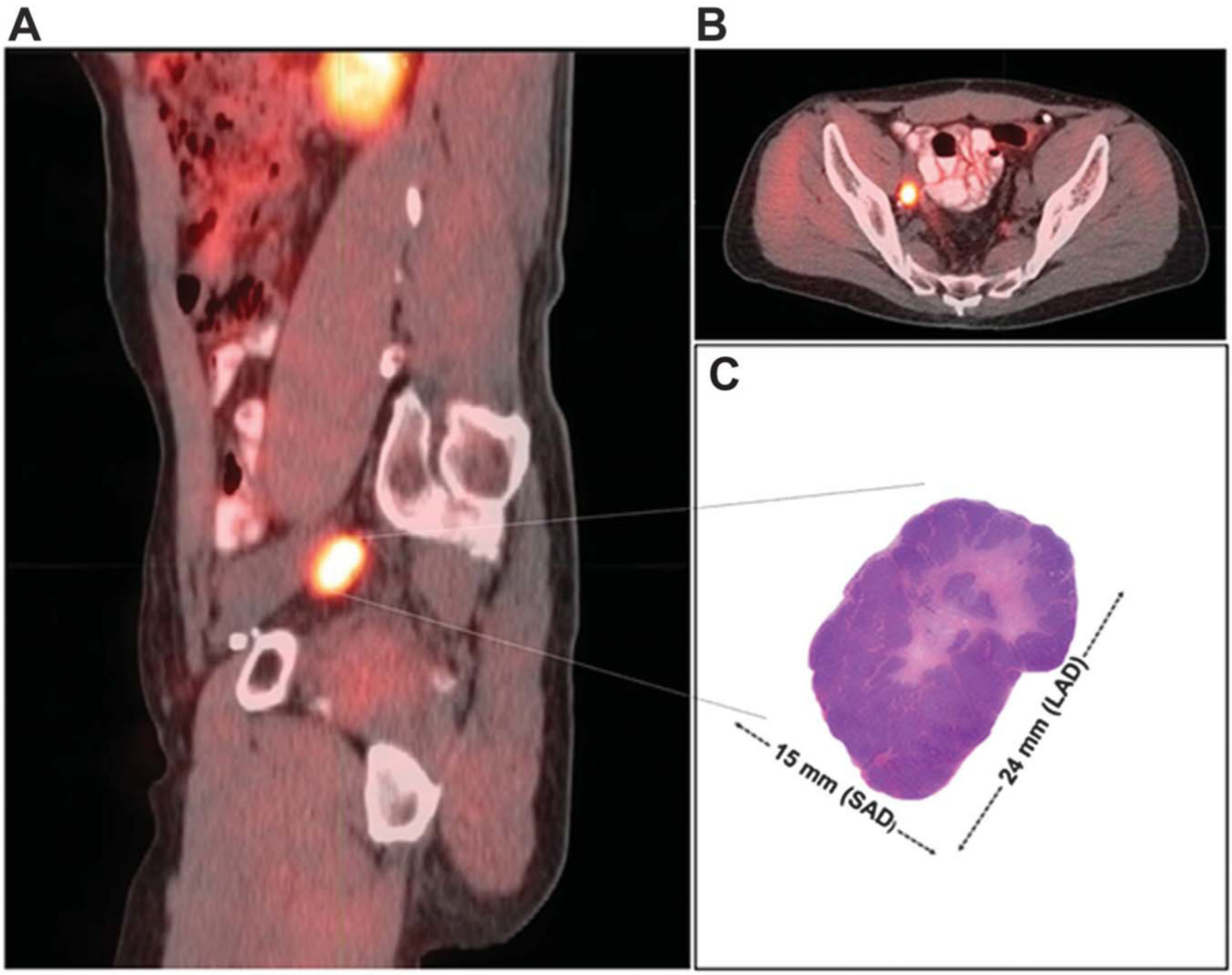

Figure 1.

^{11}C-acetate PET/CT image matched lymph node histology. *A*, sagittal view shows avid right external iliac lymph node (level I) with 19 in LAD and 14mm SAD.*B*, axial view of right external iliac lymph node. *C*, excised right external iliac lymph node with 24mm LAD and 15 mm SAD.

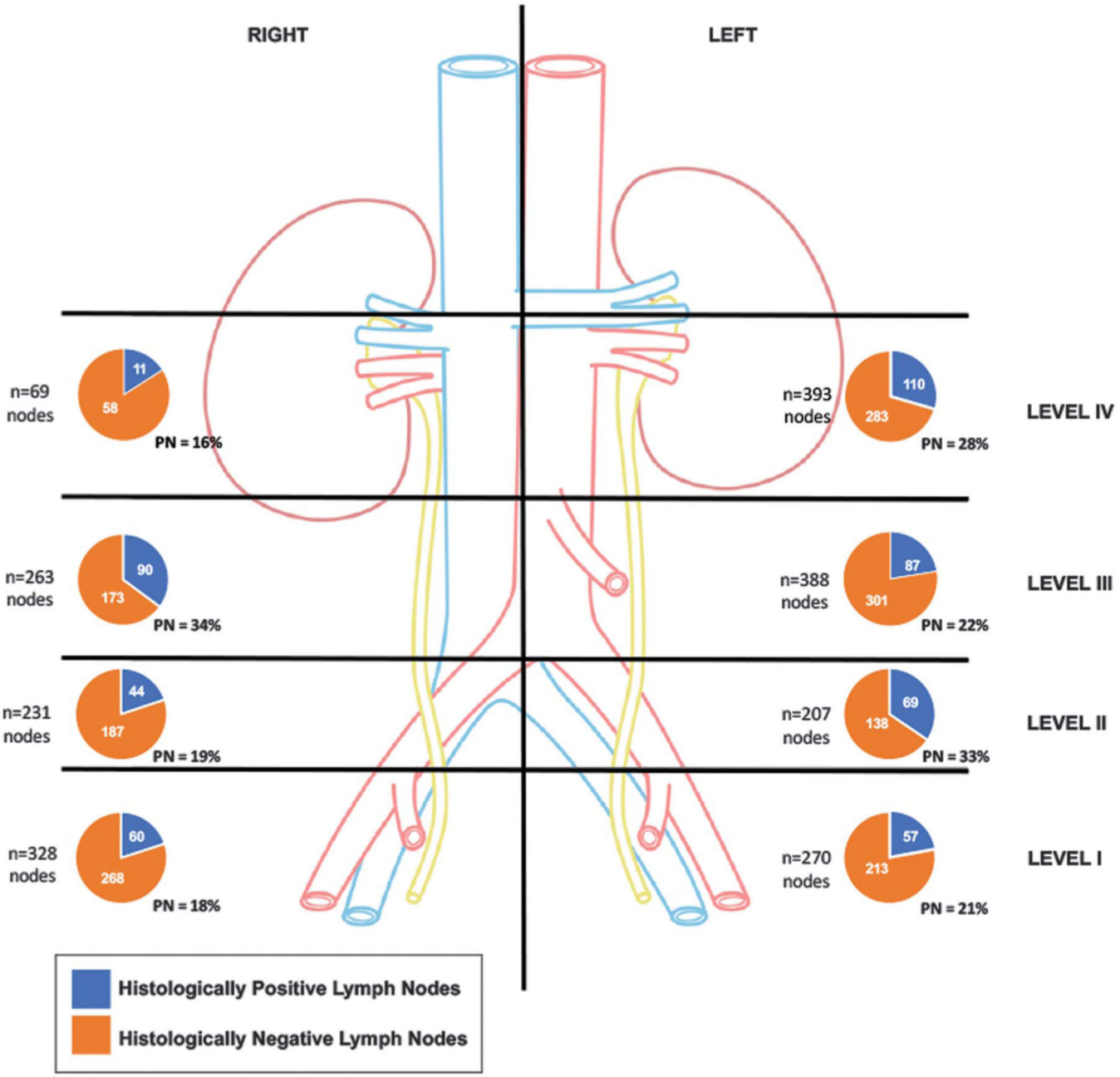

Figure 2.

Region based distribution of lymph nodes excised at rPLND plus rRPLND. Of 2,149 lymph nodes excised 528 demonstrated presence of metastatic prostate cancer.

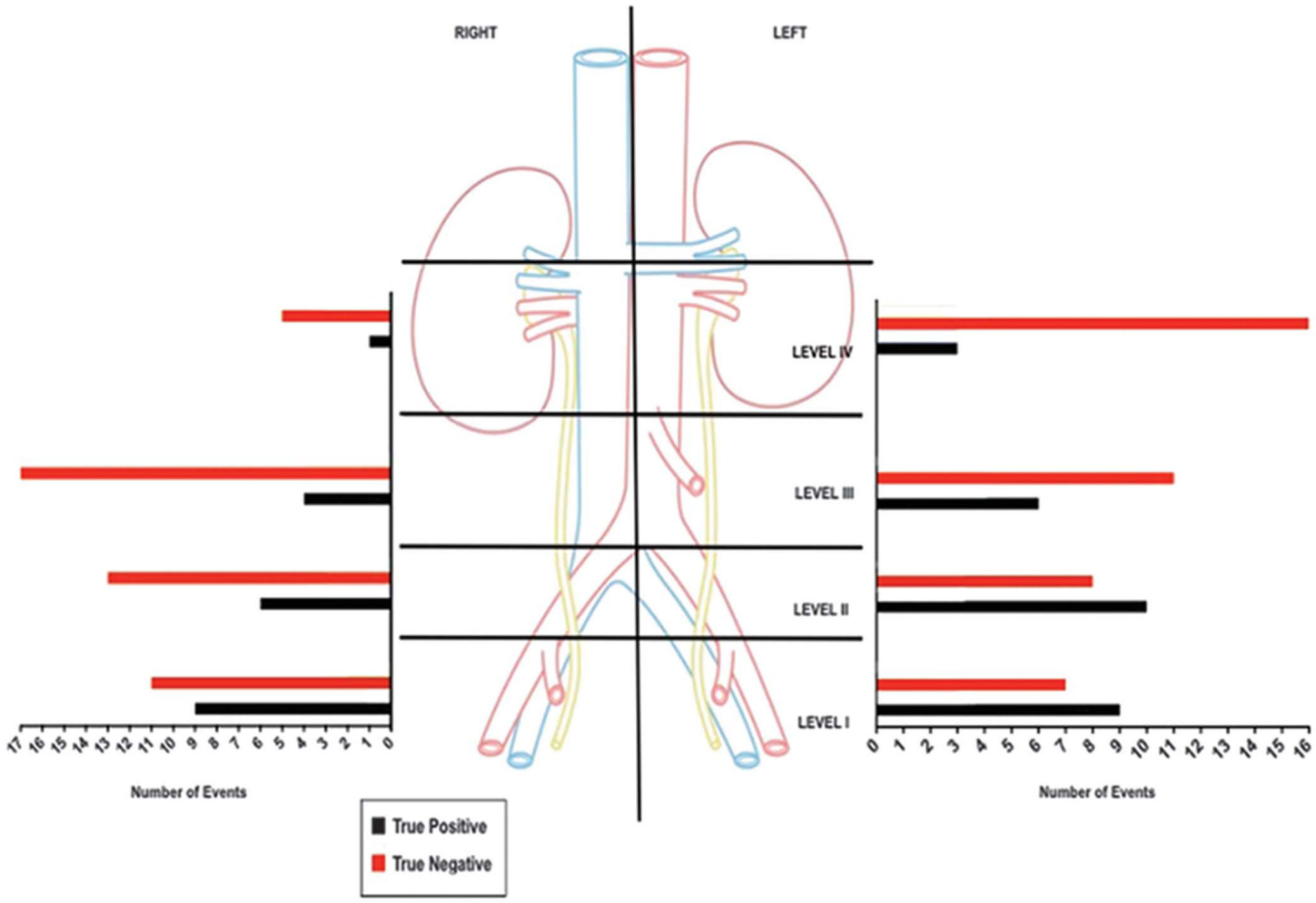

Figure 3.

Region based accuracy of ^{11}C-acetate PET/CT. Correlation of ^{11}C-acetate PET/CT findings with histopathological assessment allowed for validation per each matched region.

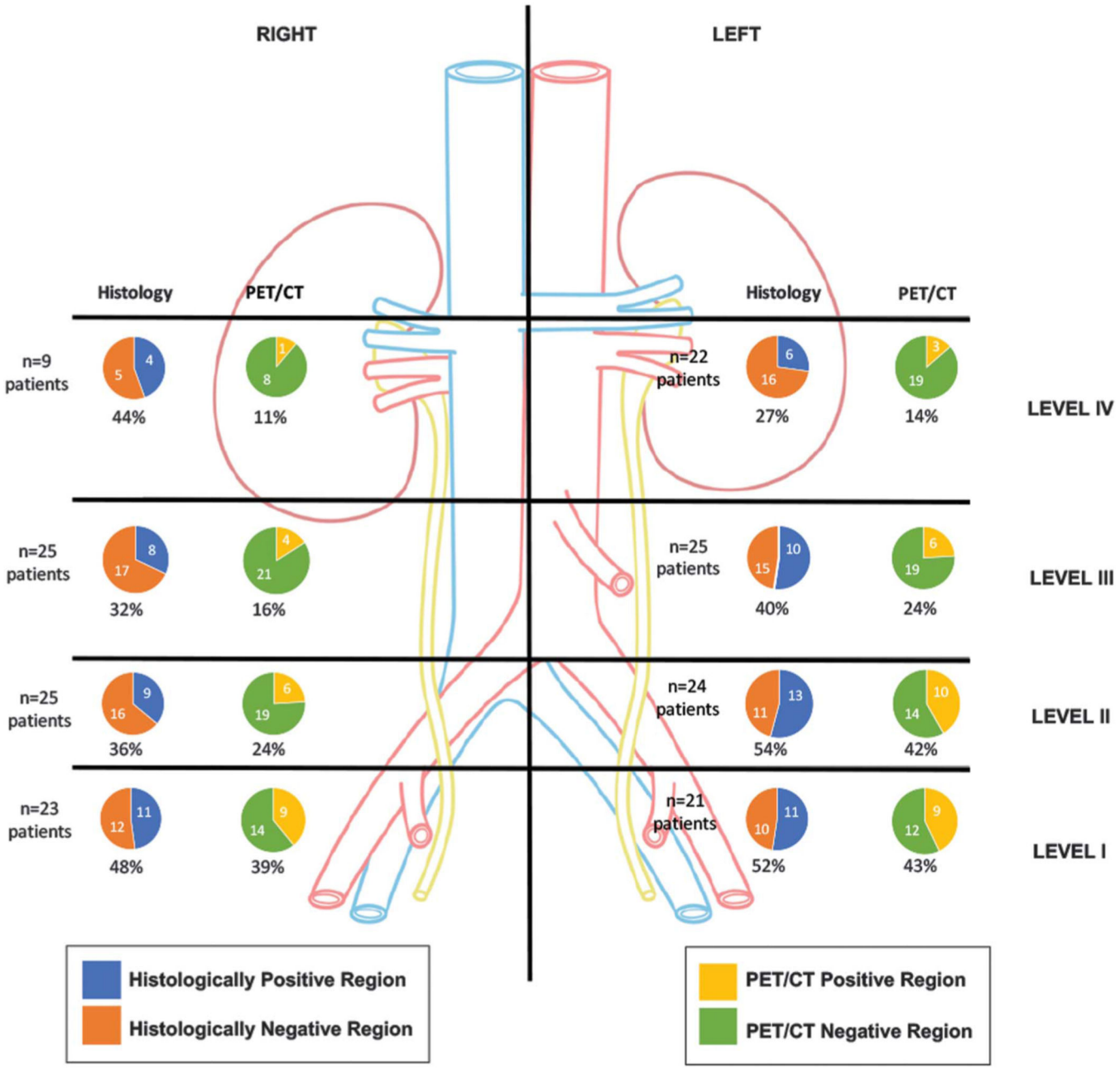

Figure 4.

Patient based analysis comparing ^{11}C-acetate PET/CT with histological findings showing detection rate by imaging modality in patients with matched imaging and histological results.

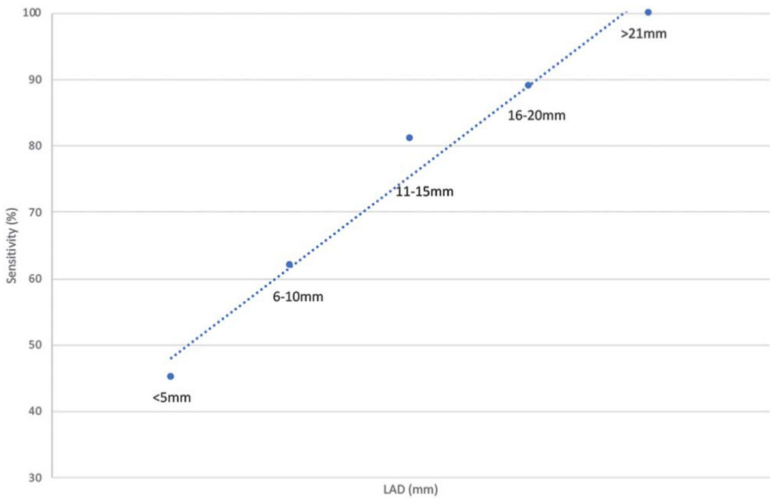

Figure 5.

Linearrelationship between ^{11}C-acetatePET/CTsensitivity and histologically positive lymph node size (long axis diameter).

Table 1.

Patient demographics, and PET/CT and surgical outcomes

No. sample pts	25	
Median age (range)	66	(46—78)
Median kg/m^2 body mass index (range)	27	(22—34)
Median American Society of Anesthesiologists™ score (range)	3	(2—4)
No. surgery:	25	
Only rPLND + rRPLND *	21	
rPLND, rRPLND + primary radical prostatectomy	1	
rPLND, rRPLND + salvage prostatectomy after failed radiotherapy	3	
Median ng/ml PSA before prostatectomy (range):	8.8	(2.1—43)
Primary prostatectomy	6.7	(2.1—43)
Salvage prostatectomy	10	(18—33)
No. prostatectomy Grade Group/Gleason score (%):		
II/3 + 4	2	(9)
III/4 + 3	10	(45)
IV/3 + 5, 4 + 4	2	(9)
V/4 + 5, 5 + 4	7	(32)
Not reported, severe radiation effect	1	(5)
No. prostatectomy pT stage (%):		
pT2a	1	(5)
pT2c	6	(27)
pT3a	9	(41)
pT3b	6	(27)
No. prostatectomy invasion present (%):		
Lymphovascular	7	(32)
Perineural	20	(91)
No. prostatectomy pos surgical margin (%)	4	(18)
Median % prostate occupied by tumor (range)	15	(5—20)
No. transrectal ultrasound biopsy Grade Group (Gleason score):	3 *	
III (4 + 3)	1	
IV (4 + 4)	1	
V (4 + 5)	1	
Median ng/ml PSA before PET/CT (range)	3.8	(0.3—32.6)
Median mos PSA doubling time (range)	4.8	(—4.6—19.4) †
Median days PET/CT to rPLND + rRPLND (range)	42	(9.0—163.0)
No. androgen deprivation therapy cases at PET/CT (%)	4	(16)
No. LNs excised at rPLND + rRPLND:		
Total	2,149	
Mean/pt (range)	86	(27—132)
No. histologically pos LNs at rPLND + rRPLND:		
Total	528	

Mean/pt (range)	21	(0—109)

*Patients did not undergo salvage prostatectomy after radiotherapy failure and only underwent rPLND and rRPLND so that prostate gland was still in situ.

†Negative due to androgen deprivation therapy with resultant downward trending PSA.

Table 2.

PET/CT corroboration with LN histology by anatomical template level, and in pelvis and retroperitoneum

			% Predictive Value	
	% Sensitivity	% Specificity	Pos*	Neg
Level:	67	84	74	79
I	82	82	82	82
II	73	78	78	78
III	56	88	71	78
IV	40	100	100	78
Pelvis (levels I-II)†	77	80	77	80
Retroperitoneum (levels III-IV)	50	88	67	78

*Per patient 84% and since rPLND was not done in patients with negative PET/CT sensitivity, specificity and negative predictive value at patient level could not be determined but by region PET/CT sensitivity decreased with more cephalad levels.

†PET/CT was more accurate in pelvis than in retroperitoneum.

Table 3.

Correlation of PET/CT image and histology results (Mann-Whitney non-parametric test)

	TP Median (range)		FP Median (range)		p Value
Comparison of PET/CT parameters of true positive and false-positive images *					
PET/CT LAD (mm)	9.5	(1.2–40)	8.5	(1.2–22)	0.2
PET/CT SAD (mm)	8	(1–23)	7	(1.1–17)	0.1
SUV	3.2	(1.2–12.4)	2.3	(1.4–3.9)	0.006
Correlation of histological findings with true positive and false-negative PET/CT images †					
LAD of cancer bearing lymph node (mm)	12	(2–27)	8.5	(2–22)	0.02
SAD of cancer bearing lymph (mm)	6	(2–23)	4	(2–12)	0.0003
LAD of metastatic lesion within lymph node (mm)	11	(0.5–27)	5.5	(0.1–17)	0.002
SAD of metastatic lesion within lymph node (mm)	6	(0.1–23)	3	(0.1–12)	<0.0001
Extranodal extension (%)	88		58		0.004
Comparison of histological lymph node size of true positive and true negative PET/CT images					
LAD of cancer bearing lymph node, (mm)	12	(2–27)	9	(1–22)	0.02
SAD of cancer bearing lymph node, (mm)	6	(2–23)	4	(1–18)	<0.0001

*SUV reading can be available only for true-positive and false-positive images; negative PET/CT images do not report SUV readings.

†Pathologically confirmed cancer cells within lymph nodes can be seen only on true positive and false-negative images, and patients with true negative and false-positive PET/CT images cannot have cancer cells in their pathology.

Table 4.

Ability of ^{11}C-acetate PET/CT to detect histologically positive nodes based on lymph node long axis diameter

Ca Bearing Node Long Axis Diameter (mm)	% Sensitivity (No. LNs/total No.)
5 or Less	45 (10/22)
6—10	62 (13/21)
11—15	81 (13/16)
16—20	89 (8/9)
21 or Greater	100 (4/4)